UDC 544.03 DOI: 10.18698/1812-3368-2022-6-157-173

ELECTRONIC STRUCTURE AND OPTOELECTRONIC PROPERTIES OF A NEW POLYMER SERIES (N-ALKYL 2-PYRIDONE DITHIOPHENE) PDTs

D.M. Mamand[1] dyari.mustafa@uor.edu.krd
T.H. Rasul[1]
A.H. Awla[1]
T.M.K. Anwer[2]

[1] **University of Raparin, Sulaymaniyah, Iraq**
[2] **Salahaddin University, Erbil, Iraq**

Abstract

One of the most important factors in life today is energy and how to get it. Different methods are used to develop low-cost, high-performance materials for electrical devices such as solar cells. In this paper, some properties of three polymer materials are investigated. Through the use of UV-visible spectrum, we have been able to discover several properties that help determine the level of materials in terms of electrical and electronic devices. Based on *Gaussian 09* software, and geometries of all the studied polymers compounds were fully optimized and established on density functional theory with functional B3LYP, which has evolved very favored in current decades. Several quantum chemical properties were investigated and compared with other polymer properties, such as stiffness, flexibility, electronegativity, bandgap energy, ionization potential, chemical potential, electron back donation and electron transport

Keywords

Optoelectronic, UV-vis spectrum, HOMO, LUMO, MEP

Received 30.05.2022
Accepted 21.06.2022

Introduction. The word polymer is derived from the classical Greek phrase's poly meaning many, and meres meaning parts [1]. A polymer is a long chain molecule consisting of a number of repeating units with the same structure. Some polymers, such as proteins, cellulose, and silk, occur naturally in nature. Many polymers, such as polystyrene, polyethylene, and nylon, can only be made synthetically. Certain natural polymers can also be synthesized [2, 3]. Natural rubber (Hevea), also known as polyisoprene in its synthetic version, is a good example [4]. As elastomers, polymers with great extensibility under ambient circumstances have vital applications. In addition to natural rubber, synthetic elastomers such as nitrile and butyl rubber are essential [5]. Other polymers may

have properties that allow them to be formed into long strands suited for textile applications. Synthetic fibers, primarily nylon and polyester, are excellent alternatives for natural fibers such as cotton, wool, and silk. In contrast to the term polymer, commercial products developed from synthetic polymers other than elastomers and fibers are referred to as plastics [6, 7]. In addition to different additives and fillers, a typical commercial plastic polish may comprise two or more polymers. These are used to enhance a certain attribute, such as processability, mechanical qualities, and environmental stability. Recent advances in research on organic solar cells, particularly those based on polymers, have shown promise as a green technology for converting solar energy into electricity [8, 9]. This advancement is being driven by multidisciplinary research improvements spanning from new material synthesis to inventive new device architectures and a deeper understanding of device physics. This attempt has resulted in devices with power conversion efficiencies, optoelectronic characteristics, and electrical structure as critical efficiency parameters that surpass 5 % in both single and tandem bulk heterojunction device topologies [10]. One of the most difficult issues in inorganic photovoltaic systems is achieving optimal sunlight absorption in the active layer, particularly in the near-infrared range. From a materials engineering standpoint, this may be done by creating polymers with narrow bandgaps that prolong light-harvesting throughout a wide range of the solar spectrum [11]. Indeed, several narrow bandgap polymers have been produced as a result of considerable international study, and have played a vital role in reaching high solar cell efficiencies and supplying key materials for device optimization research [12, 13].

In this study, we report the properties of a new series of wide bandgap photovoltaic polymers based on the N-alkyl 2-pyridone dithiophene (PDT) unit (Fig. 1) [10]. These polymers are effective bulk heterojunction solar cell materials had been blended with phenyl-C71-butyric acid methyl ester (PC71BM) and this unit had been derives success with fused amide-linked systems to create the thieno [2',3',5',6']pyrido[3,4-g]thieno[3,2-c]isoquinoline-5,11(4H,10H)-dione (TPTI) monomer for use in polymeric acceptor systems [10].

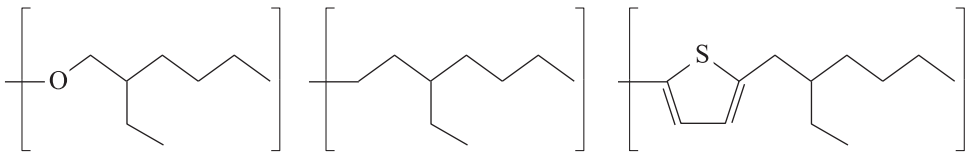

Fig. 1. Chemical structures of PPDT series polymers, N-alkyl 2-pyridone dithiophene (PDT)

UV-visible spectrum. Figure 2 depicts the UV-visisible absorption spectra of polymer films, to calculate the optical properties of the selected molecules received. Because of their comparable backbones, the PPDT 1–3 polymers exhibit similar optical spectra, with only modest red is detected in the absorption peaks of PPDT 3, probably due to enhanced conjugation with the extra thiophene moieties in the orientation perpendicular to the conjugated backbone.

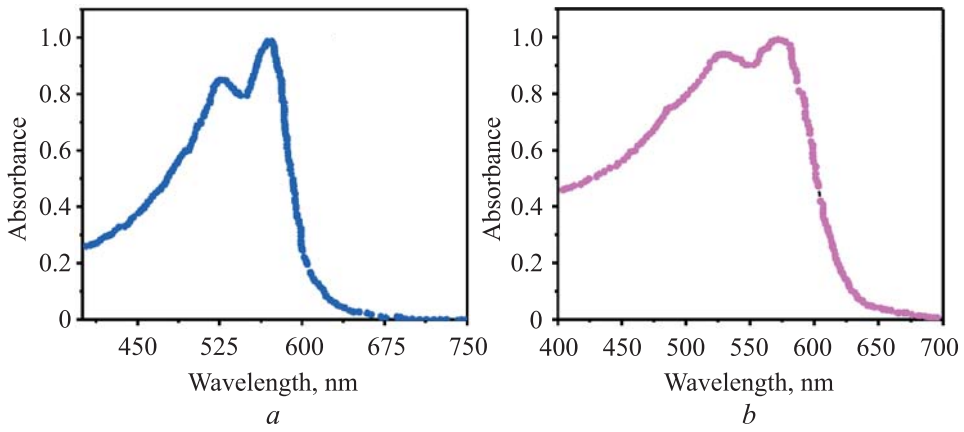

Fig. 2. UV-visible spectrum of PPDT 1 (*a*), PPDT 2 (*b*), and PPDT 3 (*c*) [10]

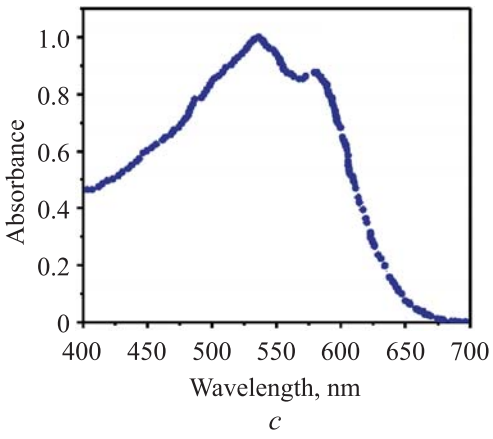

Figure 2 is the comparison between the UV-visible spectrum of PPDT 1, PPDT 2, and PPDT 3 in addition, we found that PPDT 2 material has the most absorption at a wavelength of 575 nm and has the highest absorption in maximum wavelength, and PPDT 1 and PPDT 3 have the highest absorption in minimum wavelength 575.8, 568.5, 535.4 nm (Table 1). An electron is induced from an even orbital to an antibonding orbital that becomes empty. Each jump requires energy from the light, and a higher jump requires more than a little one. Each wavelength of light is related to a specific amount of energy. If the amount of energy is absolutely perfect for one of these energy jumps, the wavelength is absorbed — its energy has been used to promote an electron. Pi bonds or atoms with non-bonding orbitals must be present in the molecule. Remember that a non-bonding orbital is a single pair on an element such as oxygen, nitrogen, or halogen. Non-bonding

orbitals have more energy than pi bonding orbitals. That is, the transition from an oxygen lone pair to a pi anti-bonding orbital requires less energy. That is, it absorbs light with a lower frequency and hence a longer wavelength [14, 15].

Table 1

Calculation the relation between absorbance (%) and wavelength (nm) with energy (eV)

Parameter	PPDT 1	PPDT 2	PPDT 3
Wavelength, nm	568.5	575.8	535.4
Energy, eV	2.1809094	2.15326	2.3157397

Absorption and transmission. The amount of light of a given wavelength that a given material prevents from travelling through is measured as absorbance. Chemical concentration and path length are the two main elements affecting absorption [16].

The polarity of the solvent has a significant effect on position and density. The position and form of the UV-Vis absorption bands are affected by a sample solution's (pH), temperature and concentration. The selected molecules in this study have been used in the solar cell due to their high bandgap energy [17]. The optical properties of solar cells are one of the most important variables determining their performance. As a result, the majority of light is reflected and passes through the solar cell, resulting in reduced inefficiency.

Light absorption can occur when light travels through an optical barrier. The degree of absorption will be the same inside and outside of the material. The absorption coefficient of materials may be calculated using extinction coefficient correlations and the Maxwell and wave equations [17]: $\alpha = 4\pi k / \lambda$, where α represents the absorption coefficient; k is the extinction coefficient of the solute material; λ is the wavelength. These coefficients are related to losses of energy.

Figure 3, *a* relates to the PPDT 1 molecule. When the bandgap energy is at its lowest energy of 1.8 eV, the conductivity is at the highest level (99.9 %). When the energy is at the highest point of 3 eV, the transition is at the lowest point and about 0. Figure 3, *b* shows the relationship between the band gap energy and the transition of the PPDT 2 molecule. When the energy is at the lowest point of 1.4 eV, the transmission of light is at its highest (100 %). When the energy stabilizes at the highest point of 3.0 eV, the transmittance of light is at its lowest point approximately (0). If the bandgap is too high, most sunlight photons cannot be absorbed, if it is too low, then most photons have much more energy than necessary to excite electrons across the bandgap, and the rest is wasted.

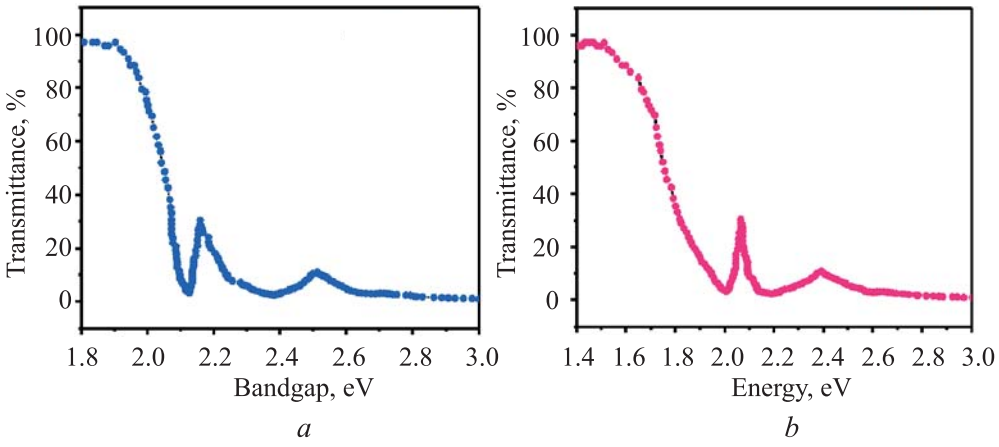

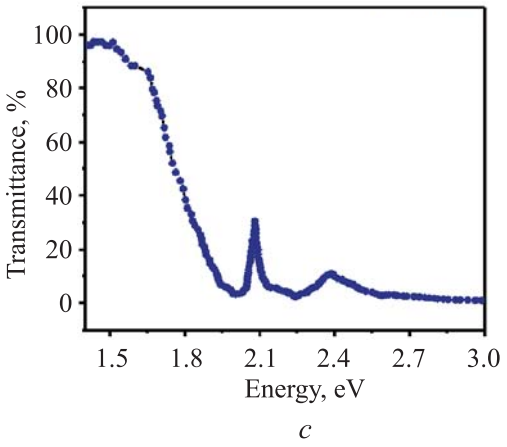

Fig. 3. Transmittance and energy gap of selected polymers PPDT 1 (*a*), PPDT 2 (*b*), and PPDT 3 (*c*)

The relationship between the bandgap energy and light transmission for the PPDT 3 polymer is shown in Fig. 3, *c*. When the energy gap is at its lowest point (0), the transmittance of photon is at its highest level of 99.9 %, and then when the energy levelincreases, the transmittance of photon decreases, resulting in an energy gap of 2.1 eV with a transmittance ratio of 30 %. The energy is stable, and when the energy gap is at its peak point of 3 eV, the transmission is at its lowest point of around 0.

Refractive index. The refractive index n is used to calculate the transparency of the material. It is a significant parameter in the physical and chemical properties of materials. The refractive index of materials should be considered when designing an optoelectronic device [18]. The variable refractive index is closely connected to the band structure and electronic properties of the material. Theoretically, two approaches are used to compute the refractive index of substances. The first approach computations linked the material's molar volume to its electrical behavior in terms of local fields. The growth of a solar cell's refractive index affects photoconversion efficiency. The refractive index grading will improve, and the reflectance will be substantially lower. This has the direct effect of increasing the photoconversion efficiency of solar cells. Nanomaterials

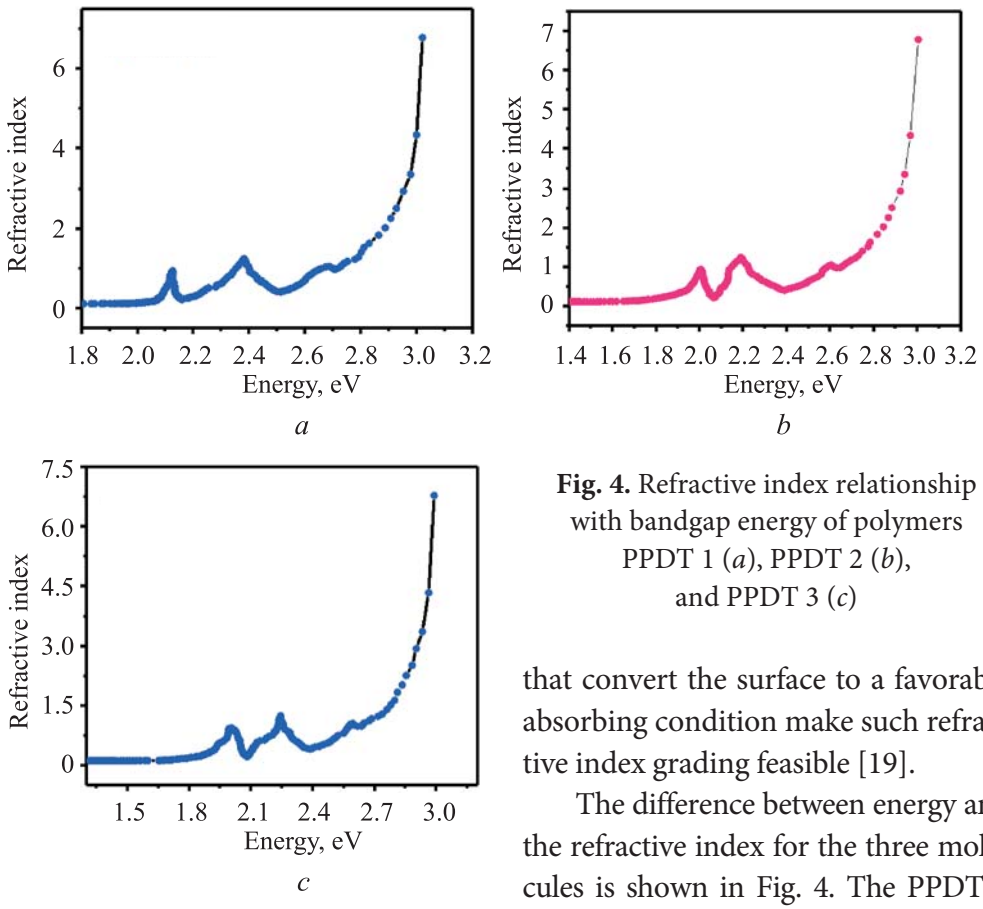

Fig. 4. Refractive index relationship with bandgap energy of polymers PPDT 1 (*a*), PPDT 2 (*b*), and PPDT 3 (*c*)

that convert the surface to a favorable absorbing condition make such refractive index grading feasible [19].

The difference between energy and the refractive index for the three molecules is shown in Fig. 4. The PPDT 1 molecule starts with an energy of 1.8 eV and a refractive index of zero. The energy gap increased until 2.85 eV with two small peaks and then increased directly upward. Concerning the PPDT 2 molecule, it starts at 1.4 eV with zero refraction and increases the energy until it reaches the peak energy of 2.2 eV, which corresponds to a refractive index of 1.5. The refractive index reaches its highest point of 6.9 when the energy exceeds 3 eV. The energy gap of the PPDT 3 starts at 0, and the refractive index is still zero, but as the energy gap increases, the peaks appear at 2.3 eV, and the refractive index rises to 1.5. The refractive index reaches its greatest point of 7.1 when energy strikes 3 eV.

Optical and electrical conductivity of selected polymers. The most significant properties of materials, optical and electrical conductivity, can be calculated using the following equations [20, 21]:

$$\sigma_{opt} = \frac{\alpha nc}{4\pi}; \quad \sigma_{el} = \frac{2\lambda\sigma_{opt}}{\alpha}.$$

Here c indicates the velocity of light. Materials' electrical conductivity is caused by free electrons in the conduction band, whereas semiconductor optical

conductivity is the change in conductivity caused by light, which can be either a reduction or an increase. The electrical conductivity of materials may be explained using Drude's model [21]. As the overlap between the conduction band and the valence band began to receive more free electrons in the conduction band, band theory became essential. Because of the so-called scattering process, excited electrons from the valence band to the conduction band are responsible for conduction, and the material has resistance [22]. Optical conductivity is the electrical conductivity measurement in an electro-magnetic field [23]. It is necessary to consider the dielectric constant since it is related to the propagation of light into the material. The relaxation time and plasma frequency are the most significant characteristics to consider and should consider. In the case of optical scattering, these two physical quantities are required. When light energy in the form of a photon strikes the surface of a material it drives the electron, and if there is no scattering, the light is completely reflected, which is why metals appear shiny. This aspect has to do with the color of the materials.

The dielectric constant of the materials correlated with the complex optical conductivity can express from the following relationships [24]: $\varepsilon_r = n^2 - k^2$; $\varepsilon_i = 2nk$, where n and k indicate the refractive index and extinction coefficient. The relationships between the bandgap energy with the real (ε_r) and imaginary (ε_i) part of PPDT 1, are shown in Fig. 5. In the lowest frequency, the real fraction of photoconductivity is zero in the lowest bandgap energy and the highest value is observed at 2.2 eV. Initially, both of them decreased with an increase in the frequency and energy, in the range of 2.4 eV, and indicates a small peak and increased about $7 \cdot 10^3$ S, and then both decreased with increasing frequency and continued to be close to zero after 2.8 eV.

The relationships between the angular frequency with the optical and electrical conductivity PPDT 2 are shown in Fig. 6. The optical conductivity is zero in the lowest angular frequency and the highest value observed at $3.3 \cdot 10^{15}$ S. When optical conductivity is $2.3 \cdot 10^7$ S, the electrical conductivity is $3.9 \cdot 10^9$ S in the lowest angular frequency, and the highest value observed at $3.3 \cdot 10^{15}$ when electrical conductivity is $1.2 \cdot 10^{10}$ S. Initially, both increased with angular frequency and acquired two peaks and then both decreased with increasing frequency.

At the lowest energy gap, the real part of the dielectric constant is zero, and the highest value is obtained at 2.2 eV. Initially, the actual and imaginary parts grow with a growing energy gap, resulting in two peaks. They observed tiny peaks in the 2.2 and 2.4 eV bands, and then both declined with increasing power to 3 eV.

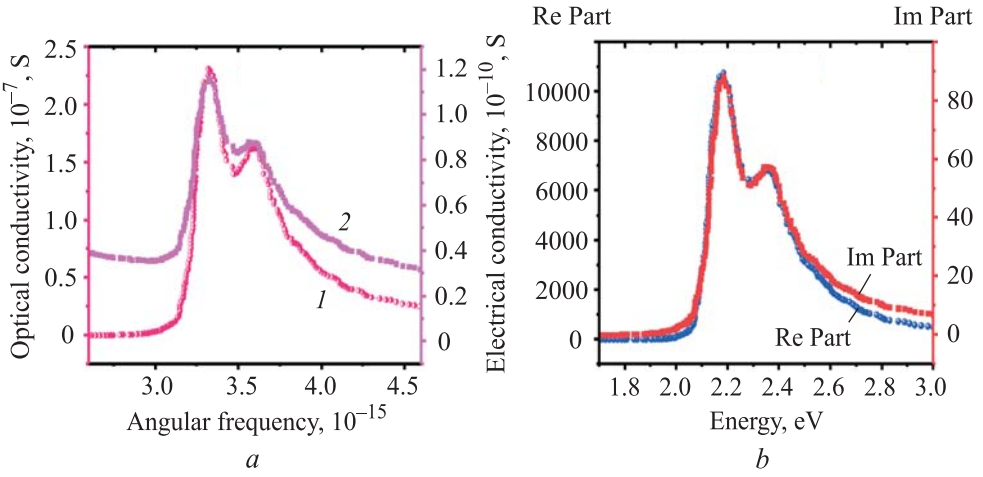

Fig. 5. Electrical (*1*) and optical (*2*) conductivity of PPDT 1 molecule (*a*), and real and imaginary part of dielectric constant (*b*)

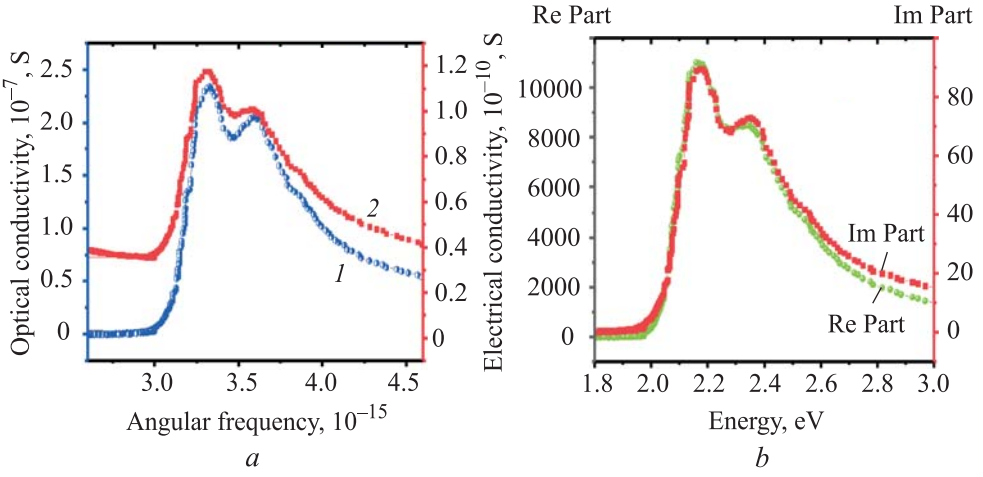

Fig. 6. Electrical (*1*) and optical (*2*) conductivity of PPDT 2 molecule (*a*), and real and imaginary part of dielectric constant (*b*)

The energy correlations with the dielectric constants of the real and imaginary parts of the PPDT 3 molecule shows Fig. 7. The real part is zero at the lowest energy, while the energy gap is 2.3 eV and the highest value obtained from the real dielectric constant. Initially, they increased with increasing energy gap forming two peaks in the 2.1 and 2.3 eV.

Electrical susceptibility. The capacity of materials to polarize is connected to their electrical susceptibility; a greater value of χ_e implies a more polarized material, which increases the overall electric field inside the material, and vice versa [25, 26]: $\chi_e = \varepsilon_r - 1$.

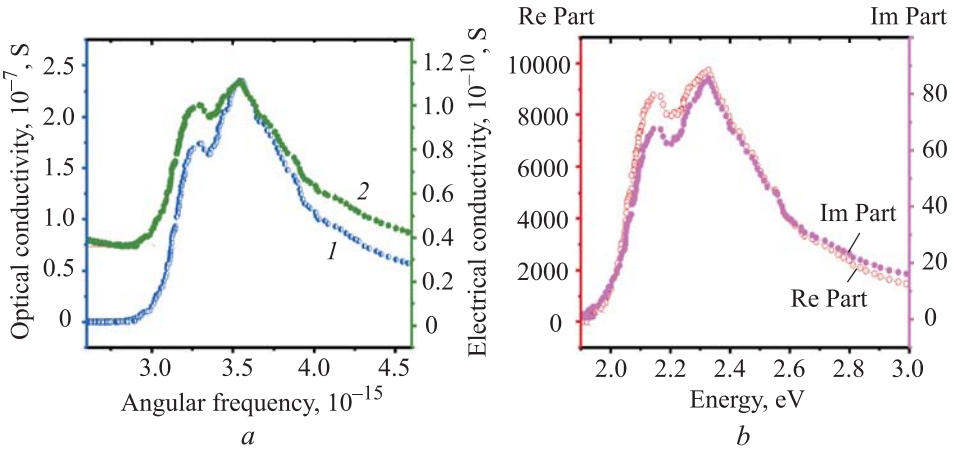

Fig. 7. Electrical (*1*) and optical (*2*) conductivity of PPDT 3 molecule (*a*), and real and imaginary part of dielectric constant (*b*)

The capacity of a material to improve transient polarization or all of it is measured by dielectric susceptibility χ_e, and linear electrical susceptibility (Fig. 8) may be calculated using the following calculation: $\chi_e = (\varepsilon_r - 1)/(4\pi)$.

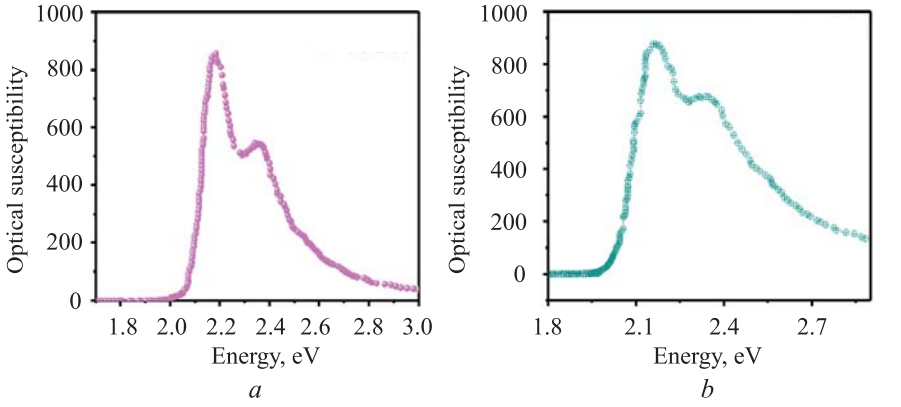

Fig. 8. The relation between optical susceptibility and energy of polymers PPDT 1 (*a*), PPDT 2 (*b*), and PPDT 3 (*c*)

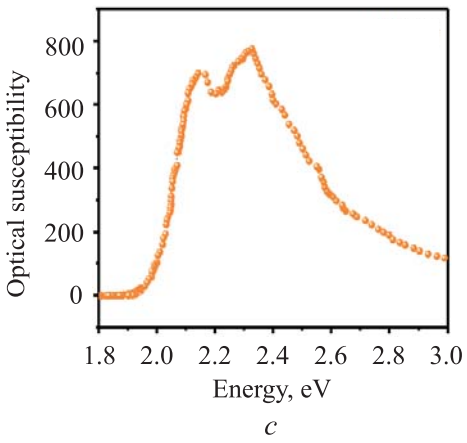

X-ray scattering data. In this study, we were able to discover some properties of materials thanks to UV radiation. However, to become more familiar with the composition of these materials, we took the morphology

from the previous study. Grazing incidence wide-angle X-ray scattering (GISAXS) had been used to examine the crystalline intermolecular interactions in the polymer films to additional study morphology in this polymer series. The out-of-plane (010) $\pi-\pi$ stacking peak visible in all of the tidy films indicates the preferred p-face-on polymer backbone orientation compared to the substrate at the interface in all of the immaculate polymers (Table 2).

Table 2

GIWAXS-derived d-spacing and correlation length data calculated for pristine PPDT films

d-spacing, Å	Correlation length, nm		
	PPDT 1	PPDT 2	PPDT 3
(100)	18.6	18.5	19.6
(010)	3.96	4.02	3.86
(100)	3.2	4.2	6.0
(010)	3.0	2.1	2.7

Plane (010) $\pi-\pi$ stacking peak apparent in all the neat films. Table 2 summarizes the correlation length. Figure 9 illustrates the out-plane and in-of-plane linecuts and the d-spacing; $\pi-\pi$ stacking distance scope from 3.86 to 4.02 Å. PPDT 2 has the largest distance compare with other molecules.

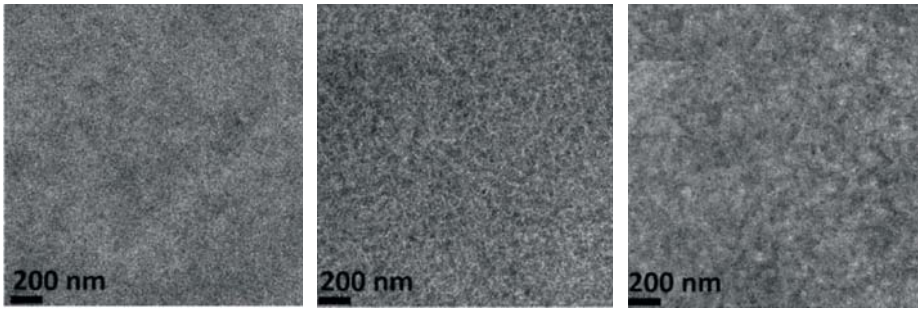

a *b* *c*

Fig. 9. TEM images of optimized PPDT 1 (*a*), PPDT (*b*), and PPDT (*c*); PC71BM devices (the scale bar in the TEM images is 200 nm)

Electronic structure. Density functional theory (DFT) is unquestionably the most commonly utilized tool for predicting molecular chemical reactivity. For all computations provided in this paper, the *Gaussian 09* software was employed (Fig. 10) [27]. In contrast, the *Gauss View 5.0.8* software was used to produce the input files for the compounds under investigation. All of the investigated compounds' geometries were thoroughly optimized using DFT with functional B3LYP, which has recently gained popularity [28].

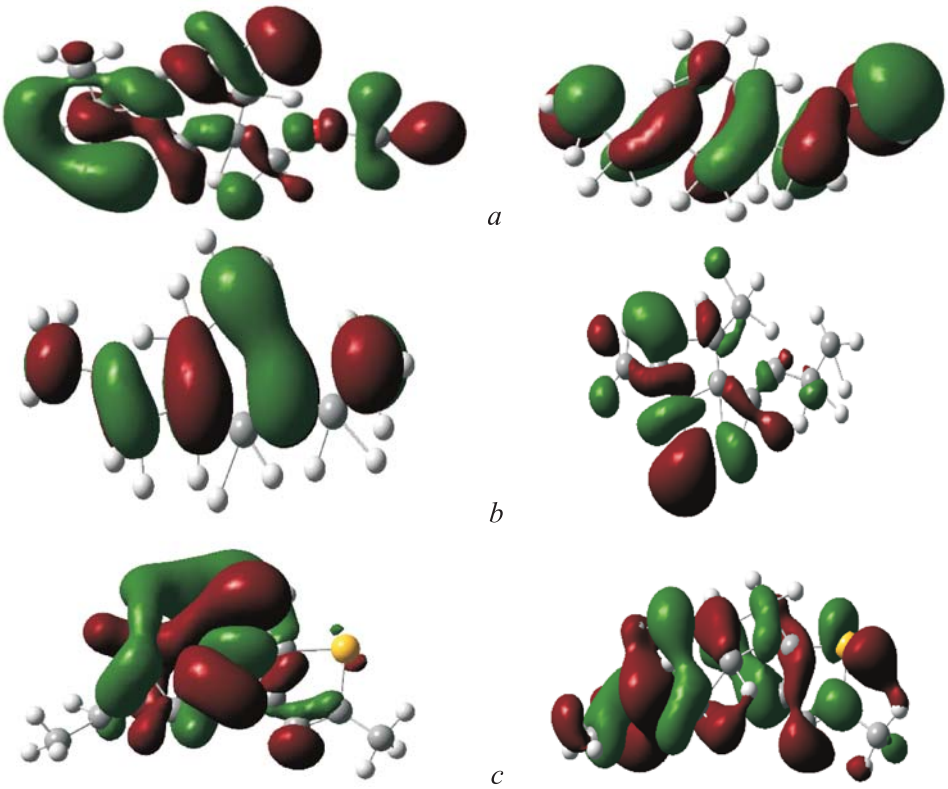

Fig. 10. Output result of *Gaussian 09* program of selected polymers PPDT 1 (*a*), PPDT 2 (*b*), and PPDT 3 (*c*) in gas phase

In recent years, it has been demonstrated that DFT methodologies can provide good additional insight into chemical reactivity indices such as chemical hardness η, energy gap (E_{gap} = HOMO – LUMO), electronegativity χ, ionization energy I, electron affinity A, chemical potential μ, proton affinity (PA), electrophilicity ω and nucleophilicity ε and selectivity, both as global and local identifiers as Fukui functions $f(r)$. Nucleophilicity ε, and electrophilicity ω are reactivity indices defined as derivatives of the number of electrons N of the electronic energy E at external potential r. The mathematical operations associated with these notions are represented by the equations below [29, 30]:

$$\mu = -\chi = \left(\frac{\partial E}{\partial N}\right)_{v(r)}; \quad \eta = \frac{1}{2} = \left(\frac{\partial^2 E}{\partial N^2}\right)_{v(r)} = \frac{1}{2}\left(\frac{\partial E}{\partial N}\right)_{v(r)};$$

$$\mu = -\chi = \left(\frac{I + A}{2}\right); \quad \eta = \left(\frac{I - A}{2}\right); \quad \sigma = \frac{1}{\eta};$$

$$\chi = -\mu = \frac{-E_{\mathrm{HOMO}} - E_{\mathrm{LUMO}}}{2};\ \ \eta = \frac{E_{\mathrm{LUMO}} - E_{\mathrm{HOMO}}}{2};\ \ \omega = \frac{\mu^2}{2\eta} = \frac{\chi^2}{2\eta}.$$

The examined polymers optimized molecular structure, molecular electrostatic potentials (ESP), HOMO, and LUMO. As is well known, applying quantum chemical simulations to construct a usable molecule structure is a critical technique. According to Fukui's hypothesis, electron transition is caused by contact between the responding species' HOMO and LUMO.

The positive number of electrons transferred shows that the molecules serve as electron acceptors, whereas the negative number of electrons transferred indicates that the molecules act as electron donors:

$$\Delta N_{\max} = \frac{\chi_{\mathrm{Fe}} - \chi_{inh}}{2\left(\eta_{\mathrm{Fe}} + \eta_{inh}\right)}.$$

The value of $\Delta N_{\max} < 3.6$ eV reflects a molecule's proclivity to give electrons. The electron transfer rates for each of the materials PPDT 1, PPDT 2, PPDT 3 as shown in Table 3 are equal to 8.332, 3.264 and 0.695. Table 3 demonstrated that chemical hardness basically represents resistance to deformation or polarization of the electron cloud of polymer molecules. Hard molecules have a big energy gap, whereas soft molecules have a tiny energy gap. Electrophilicity is a measure of a chemical species' proclivity to receive electrons. The higher the degree of electrophilicity, the greater the molecule's ability to receive electrons. As a result, a good nucleophile has low values of chemical potential. The PPDT 3 has a higher electrophilicity.

Table 3

Quantum chemical parameters of PPDT, DFT at B3LYP level and 6-311G ++G (d, p) basis set in gas phase

Quantum chemical parameter	PPDT 1	PPDT 2	PPDT 3
HOMO	–3.63680361	–0.13759	–0.25104
LUMO	–3.20740772	–0.0943	–0.21925
Ionization potential	3.636804	3.744016526	6.831149856
Electron affinity	3.207408	2.56603502	5.96609945
Band gap energy	0.429396	1.177981506	0.865050406
Hardness	0.214698	0.588990753	0.432525203
Softness	4.657706	1.697819524	2.312004001
Electronegativity	3.422106	3.155025773	6.398624653
Chemical potential	–3.42211	–3.155025773	–6.398624653

End of the Table 3

Quantum chemical parameter	PPDT 1	PPDT 2	PPDT 3
Electrophilicity	27.27275	8.450207051	47.32949336
Nucleophilicity	0.036667	0.118340296	0.021128475
Back-donation	–0.05367	–0.147247688	–0.108131301
Electron transfer	8.332391	3.264036156	0.695191104
Initial molecule-metal interaction energy	–14.9062	–6.275067448	–0.209035396

Electrostatic potential maps. Electrostatic potential maps (Fig. 11) are three-dimensional atomic representations. It allows us to see the charges of dispersion atoms as well as the characteristics of charging particles [31]. It also allows us to predict the size and condition of molecules. Potential maps of static electricity are meaningful in forecasting the behavior of complicated particles in natural sciences. The Molecular electrostatic potential (MEP) surface is used to find the mole-

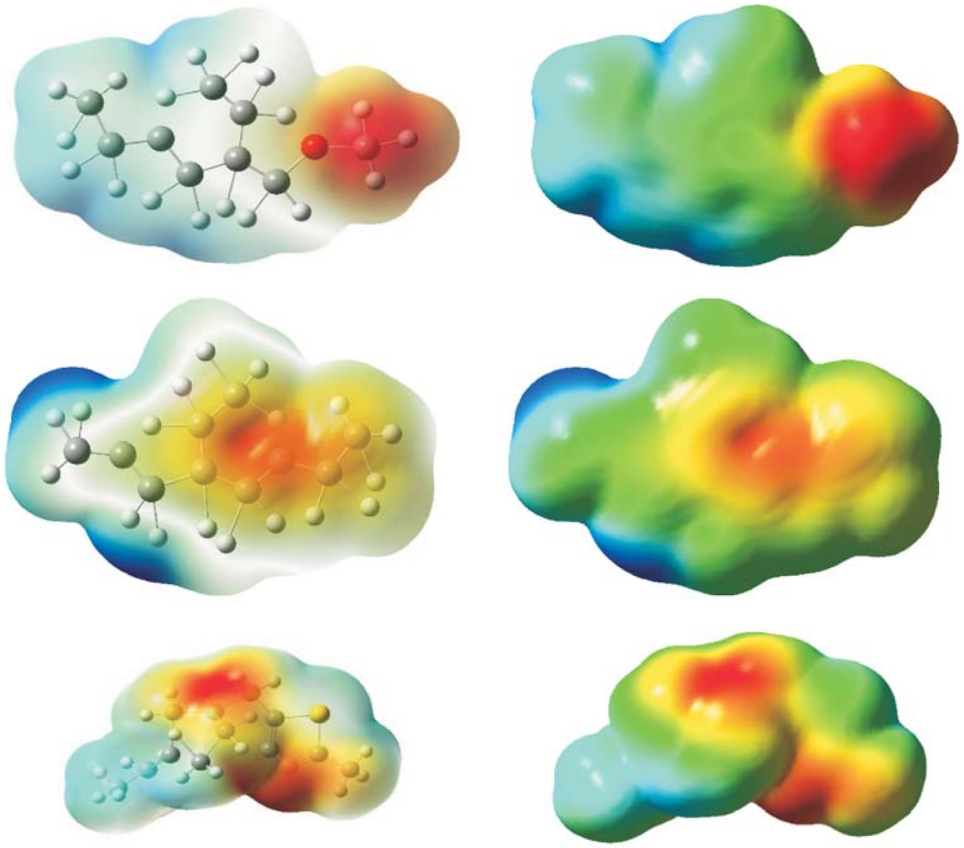

Fig. 11. Electrostatic potential map PPDT 1, PPDT 2, PPDT 3 and BBL molecule

cule's positive and negative charged electrostatic potential. As few as possible MEP surfaces have a color scale indicating negative and positive values. The red represents the negative extreme, while the blue represents the positive extreme. The red coloring with a negative sign indicates the lowest electrostatic potential (which means it is loosely bound or has surplus electrons) and acts as an electrophilic assault. The blue represents the highest electrostatic potential and acts in the opposite direction.

Red areas on a map represent the most electron-rich parts of a molecule, whereas blue areas represent the most electron-poor sections of a molecule. The red zone is near oxygen, whereas the two blue sections are near hydrogens. This suggests that the oxygen in this molecule is very electron-rich, whereas the hydrogens are somewhat electron-poor, that is true for all molecules.

Conclusion. A novel polymer series, PPDT, had been industrialized, produced, and thoroughly described based on the pyridine-thiophene unit. These materials have been used very well and successfully in electrical appliances since the bandgaps are very suitable for this purpose for each of the materials PPDT 1, PPDT 2, and PPDT 3 is equal to 2.18, 2.15, 2.31 eV. The thin film's refractive index is a crucial factor in the likelihood of total internal reflection within the solar cell. The maximum refractive index of light occurs within these materials at about 3 eV. Moreover, compared to cutting-edge narrow bandgap materials, these materials undergo a different portion of the solar spectrum, making them find applications for use in alternative polymer solar cell device topologies such as tandem or ternary cells because its electrical conductivity is equal to $1.2 \cdot 10^{10}$ S. The dielectric constant is an important parameter that affects the power conversion efficiency of organic solar cells; therefore, we calculated that the maximum amount of this property occurs between 2.2 and 2.4 eV for these polymeric materials used in this study. To investigate the electronic optical properties, based on the ultraviolet-visible spectrum, many properties such as refractive indices, transmittance, bandgap energy, electrical and optical conductivity, and dielectric susceptibility calculated. The electronic structure of the chain polymer is studied using *Gaussian 09* software, and several quantum chemical properties are determined.

REFERENCES

[1] Oberoi S., Malik M. Polyvinyl chloride (PVC), chlorinated polyethylene (CPE), chlorinated polyvinyl chloride (CPVC), chlorosulfonated polyethylene (CSPE), polychloroprene rubber (CR) — chemistry, applications and ecological impacts — I. In: *Ecological and Health Effects of Building Materials*. Springer, 2022, pp. 33–52.

[2] Sperling L.H. Introduction to physical polymer science. Wiley, 2005.

[3] Seymour R.B., Carraher Jr. C.E. Structure — property relationships in polymers. Boston, MA, Springer, 2012. DOI: https://doi.org/10.1007/978-1-4684-4748-4

[4] Rose K., Steinbüchel A. Biodegradation of natural rubber and related compounds: recent insights into a hardly understood catabolic capability of microorganisms. *Appl. Environ. Microbiol.,* 2005, vol. 71, no. 6, pp. 2803–2812.
DOI: https://doi.org/10.1128/aem.71.6.2803-2812.2005

[5] Shanks R.A., Kong I. General purpose elastomers: structure, chemistry, physics and performance. In: Visakh P., Thomas S., Chandra A., Mathew A. (eds). *Advances in Elastomers I. Advanced Structured Materials,* vol. 11. Berlin, Heidelberg, Springer, pp. 11–45. DOI: https://doi.org/10.1007/978-3-642-20925-3_2

[6] Hearle J.W., ed. High-performance fibres. Elsevier, 2001.

[7] Saba N., Tahir P.M., Jawaid M. A review on potentiality of nano filler/natural fiber filled polymer hybrid composites. *Polymers*, 2014, vol. 6, no. 8, pp. 2247–2273. DOI: https://doi.org/10.3390/polym6082247

[8] Mishra A., Bäuerle P. Small molecule organic semiconductors on the move: promises for future solar energy technology. *Angew. Chem. Int. Ed. Engl.,* 2012, vol. 51, no. 9, pp. 2020–2067. DOI: https://doi.org/10.1002/anie.201102326

[9] Wang G., Melkonyan F.S., Facchetti A., et al. All-polymer solar cells: recent progress, challenges, and prospects. *Angew. Chem. Int. Ed. Engl.,* 2019, vol. 58, no. 13, pp. 4129–4142. DOI: https://doi.org/10.1002/anie.201808976

[10] Schneider A.M., Lu L., Manley E.F., et al. Wide bandgap OPV polymers based on pyridinonedithiophene unit with efficiency > 5 %. *Chem. Sci.*, 2015, vol. 6, no. 8, pp. 4860–4866. DOI: https://doi.org/10.1039/c5sc01427a

[11] Dou L., Liu Y., Hong Z., et al. Low-bandgap near-IR conjugated polymers/molecules for organic electronics. *Chem. Rev.,* 2015, vol. 115, no. 23, pp. 12633–12665. DOI: https://doi.org/10.1021/acs.chemrev.5b00165

[12] Li G., Zhu R., Yang Y. Polymer solar cells. *Nature Photon.,* 2012, vol. 6, no. 3, pp. 153–161. DOI: https://doi.org/10.1038/nphoton.2012.11

[13] Zhang Y., Chien S.-C., Chen K.-S., et al. Increased open circuit voltage in fluorinated benzothiadiazole-based alternating conjugated polymers. *Chem. Commun.*, 2011, vol. 47, no. 39, pp. 11026–11028. DOI: https://doi.org/10.1039/c1cc14586j

[14] Mamand D. Determination the band gap energy of poly benzimidazobenzophenanthroline and comparison between HF and DFT for three different basis sets. *JPCFM*, 2019, vol. 2, no. 1, pp. 32–36.

[15] Mamand D. Theoretical calculations and spectroscopic analysis of Gaussian computational examination-NMR, FTIR, UV-Visible, MEP on 2, 4, 6-nitrophenol. *JPCFM*, 2019, vol. 2, no. 2, pp. 77–86.

[16] Mamand D.M. Investigation of spectroscopic and optoelectronic properties of benzimidazobenzophenanthroline molecule. Fen Bilimleri Enstitüsü, 2020.

[17] Calabrò M., Tommasini S., Donato P., et al. The rutin/β-cyclodextrin interactions in fully aqueous solution: spectroscopic studies and biological assays. *J. Pharm. Biomed. Anal.,* 2005, vol. 36, iss. 5, pp. 1019–1027.
DOI: https://doi.org/10.1016/j.jpba.2004.09.018

[18] Adachi S. Band gaps and refractive indices of AlGaAsSb, GaInAsSb, and InPAsSb: key properties for a variety of the 2–4-μm optoelectronic device applications. *J. Appl. Phys.*, 1987, vol. 61, iss. 10, pp. 4869–4876. DOI: https://doi.org/10.1063/1.338352

[19] Boccard M., Despeisse M., Escarre J., et al. High-stable-efficiency tandem thin-film silicon solar cell with low-refractive-index silicon-oxide interlayer. *IEEE J. Photovolt.,* 2014, vol. 4, no. 6, pp. 1368–1373.
DOI: https://doi.org/10.1109/JPHOTOV.2014.2357495

[20] Mamand D.M., Qadr H.M. Comprehensive spectroscopic and optoelectronic properties of BBL organic semiconductor. *Prot. Met. Phys. Chem. Surf.,* 2021, vol. 57, no. 5, pp. 943–953. DOI: https://doi.org/10.1134/S207020512105018X

[21] Orek C., Gündüz B., Kaygili O., et al. Electronic, optical, and spectroscopic analysis of TBADN organic semiconductor: Experiment and theory. *Chem. Phys. Lett.*, 2017, vol. 678, pp. 130–138. DOI: https://doi.org/10.1016/j.cplett.2017.04.050

[22] Elci A., Scully M.O., Smirl A.L., et al. Ultrafast transient response of solid-state plasmas. I. Germanium, theory, and experiment. *Phys. Rev., B*, 1977, vol. 16, iss. 1, pp. 191–221. DOI: https://doi.org/10.1103/PHYSREVB.16.191

[23] Grigorchuk N.I. Size and shape effect on optical conductivity of metal nanoparticles. *Europhys Lett*., 2018, vol. 121, no. 6, art. 67003.
DOI: https://doi.org/10.1209/0295-5075/121/67003

[24] Hamad T.K. Refractive index dispersion and analysis of the optical parameters of (PMMA/PVA) thin film. *Al-Nahrain J. Sci.*, 2013, vol. 16, no. 3, pp. 164–170.

[25] Waser R. Nanoelectronics and information technology: advanced electronic materials and novel devices. Wiley, 2012.

[26] Webb A. Dielectric materials in magnetic resonance. *Concepts Magn. Reson. Part A*, 2011, vol. 38, iss. 4, pp. 148–184. DOI: https://doi.org/10.1002/cmr.a.20219

[27] Qadr H.M., Mamand D.M. Molecular structure and density functional theory investigation corrosion inhibitors of some oxadiazoles. *J. Bio Tribo Corros.,* 2021, vol. 7, no. 4, art. 140. DOI: https://doi.org/10.1007/s40735-021-00566-9

[28] Mamand D.M., Awla A., Anwer T.M.K., et al. Quantum chemical study of heterocyclic organic compounds on the corrosion inhibition. *Chim. Techno Acta*, 2022, vol. 9, no. 2, art. 20229203. DOI: https://doi.org/10.15826/chimtech.2022.9.2.03

[29] Erdoğan Ş., Safi Z.S., Kaya S., et al. A computational study on corrosion inhibition performances of novel quinoline derivatives against the corrosion of iron. *J. Mol. Struct.*, 2017, vol. 1134, pp. 751–761. DOI: https://doi.org/10.1016/j.molstruc.2017.01.037

[30] Bedair M. The effect of structure parameters on the corrosion inhibition effect of some heterocyclic nitrogen organic compounds. *J. Mol. Liq.*, 2016, vol. 219, pp. 128–141. DOI: https://doi.org/10.1016/j.molliq.2016.03.012

[31] Politzer P., Laurence P.R., Jayasuriya K. Molecular electrostatic potentials: an effective tool for the elucidation of biochemical phenomena. *Environ. Health Perspect.,* 1985, vol. 61, pp. 191–202. DOI: https://doi.org/10.1289/ehp.8561191

Mamand Dyari Mustafa — Department of Physics, College of Science, University of Raparin (Main Street, Ranya, Sulaymaniyah, 46012 Iraq).

Rasul Tara Hamadamin — Department of Physics, College of Science, University of Raparin (Main Street, Ranya, Sulaymaniyah, 46012 Iraq).

Awla Awat Hamad — Department of Physics, College of Science, University of Raparin (Main Street, Ranya, Sulaymaniyah, 46012 Iraq).

Anwer Twana Mohammed Kak — Department of Physics, College of Education, Salahaddin University (Kirkuk Road, Erbil, Kurdistan Region, 44002 Iraq).

Please cite this article as:

Mamand D.M., Rasul T.H., Awla A.H., et al. Electronic structure and optoelectronic properties of a new polymer series (N-alkyl 2-pyridone dithiophene) PDTs. *Herald of the Bauman Moscow State Technical University, Series Natural Sciences*, 2022, no. 6 (105), pp. 157–173. DOI: https://doi.org/10.18698/1812-3368-2022-6-157-173